ACS OMEGA

http://pubs.acs.org/journal/acsodf

Article

Study on Start-Up Membraneless Anaerobic Baffled Reactor Coupled with Microbial Fuel Cell for Dye Wastewater Treatment

Na Liu, Yanbin Yun,* Liming Hu, Linting Xin, Mengxia Han, and Panyue Zhang

Cite This: *ACS Omega* 2021, 6, 23515−23527

Read Online

ACCESS | Metrics & More | Article Recommendations

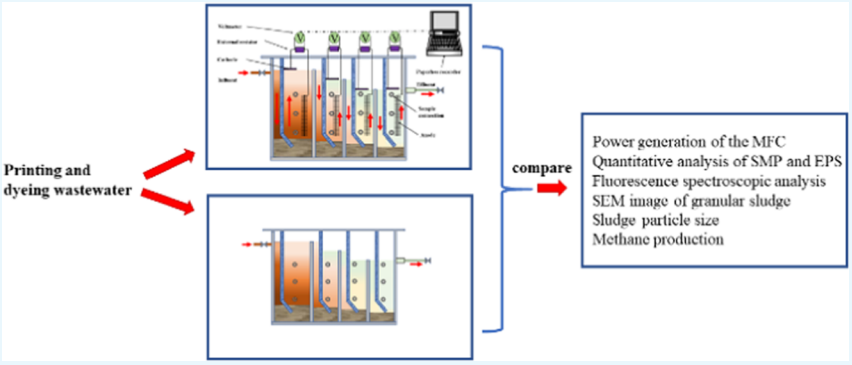

ABSTRACT: In this study, the antitoxicity performance of the traditional anaerobic baffled reactor (ABR) and the newly constructed membraneless anaerobic baffled reactor coupled with microbial fuel cell (ABR-MFC) was compared for the treatment of simulated printing and dyeing wastewater under the same hydraulic residence time. The sludge performances of ABR-MFC and ABR were evaluated on the dye removal rate, extracellular polymer (EPS) content, sludge particle size, methane yield, and the surface morphology of granular sludge. It was found that the maximum power density of the ABR-MFC reactor reached 1226.43 mW/m^3, indicating that the coupled system has a good power generation capacity. The concentration of the EPS in the ABR-MFC reactor was about 3 times that in the ABR, which could be the result of the larger average particle size of sludge in the ABR-MFC reactor than in the ABR. The dye removal rate of the ABR-MFC reactor (91.71%) was higher than that of the ABR (1.49%). The methane production and microbial species in the ABR-MFC system were higher than those in the ABR. Overall, the MFC embedded in the ABR can effectively increase the resistance of the reactor, promote the formation of granular sludge, and improve the performance of the reactor for wastewater treatment.

1. INTRODUCTION

The uneven distribution of water resources is always a great challenge in China, where water pollution that arises from the development of national economy has constantly intensified the situation.[1] According to statistics, the dye wastewater produced by the textile printing and dyeing industries in China accounts for about 20% of the industrial wastewater (36.32 billion tons) every year.[2] With the progress of printing and dye finishing technology, most of the dye compounds and their intermediate products have high biological toxicity, with carcinogenic, teratogenic, and mutagenic effects.[3−5] At present, a large volume of printing and dyeing wastewater is discharged constantly, which has a serious impact on sustainable development in China. The biochemical or physicochemical process for the treatment of printing and dyeing wastewater is not lacking in the existing literature. Although the conventional biochemical treatment may be promising, the presence of high concentrations of dye in wastewater is difficult to fully degrade.[6−8] Therefore, the development of an efficient and low-cost wastewater treatment technology is urgently needed to mitigate water pollution and recover more water resources.

Anaerobic baffled reactor (ABR) could be suitable for the treatment of high concentration of refractory organic wastewater due to its good hydraulic conditions, high load resistance, stable operation, strong adaptability, good biological distribution, less residual sludge, and simple structure.[9] However, the reaction rate of ABR is too slow and the parameters of the treated wastewater often do not meet the discharge standards. Microbial fuel cell (MFC) is an electrochemical technology that converts the chemical energy

Received: July 6, 2021
Accepted: August 23, 2021
Published: September 2, 2021

https://doi.org/10.1021/acsomega.1c03560
ACS Omega 2021, 6, 23515−23527

of the organic matter in the wastewater into electricity via a microbe electron exchange mechanism.[10,11] Recently, the MFC approach shows a strong interest in wastewater treatment due to its mild operating conditions, low operation cost, and long service life. To overcome the limitation of ABR, MFC is combined with ABR to achieve an effect of "1 + 1 > 2" by adopting the principle of microbial electricity generation to strengthen the anaerobic reactor in wastewater treatment.[12−14] This combined approach reduces the overall energy consumption and the operating cost of the conventional electrochemical method.[15,16]

The decolorization, degradation, and detoxification of azo dyes can be improved by the coupling treatment of azo wastewater with baffled anaerobic reactor and microbial fuel cell (MFC).[17] In addition, the combined approach also shows high stability and impact resistance of carbon felt filler and potential inhibition of the fouling issue in the reactor due to the special structure of the reactor.[18] On the other hand, the utilization of ABR with MFC and a microbial electrolytic cell (MEC) could realize the simultaneous removal of undesirable elements (nitrogen, carbon) and recover energy when treating wastewater. It was found that this combined process enhanced the removal rate of the chemical oxygen demand (COD) up to 99.2%.[19] Moreover, the MFC itself or in combination with other processes such as a membrane bioreacter (MBR), anaerobic fluidized bed (AFB), anaerobic−anoxic−aerobic biological nitrogen removal process (AA/O), and constructed wetland can effectively decolorize and degrade complex pollutants in wastewater, recover power, and reduce surplus sludge production simultaneously.[20−25]

Based on the above literature, it was found that the coupling of microbial fuel cells with traditional biological systems demonstrates good results in sewage treatment with minimum sludge yield and ideal energy conversion.[26,27] Therefore, this paper explored the effect of the ABR-MFC coupling reactor on the performance of activated sludge and COD removal rate under the action of a low electric field. The effects of the ABR-MFC coupling reactor and ABR were compared with the same configuration on the treatment of printing and dyeing wastewater (Figure 1).

2. RESULTS AND DISCUSSION

2.1. Power Generation of the MFC. To investigate the power generation capacity and internal resistance of the ABR-MFC coupling system, the power density curve and the polarization curve of the system were measured using the gradient transform external resistance method after the output voltage was stabilized under the condition of hydraulic residence time (HRT) of 48 h. As can be seen from Figure 2a, the power density curve decreases in the order of the second compartment > fourth compartment > third compartment > first compartment with the maximum power density of 1226.43, 953.86, 793.81, and 145.04 mW/m^3, respectively. Figure 2b shows that the trend of output voltage was in the order of second cell > fourth cell > third cell > first cell with an average output voltage at 19.87, 14.3, 12.11, and 7.38 mV, respectively.

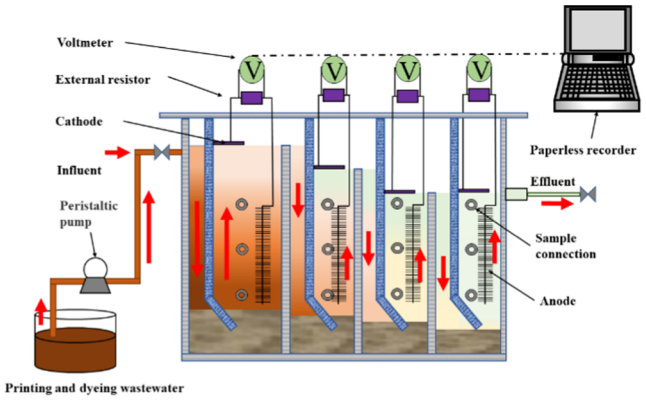

Figure 1. ABR-MFC reactor schematic diagram.

The range of the current density obtained was 49.17−209.29 mA/m^3. The findings indicated that the ABR-MFC coupling reactor can effectively utilize the organic matter in the reactor by maintaining its own growth and development, degrading pollutants, and generating electricity simultaneously. Moreover, the power density obtained was superior to that reported using the baffled reactor-bioelectricity Fenton coupling reactor (196.86 mW/m^3),[29] demonstrating the promising performance of the proposed reactor in this study.

In addition, it can be seen from Figure 2c,d that the COD removal rate and the dye removal rate of the ABR-MFC system were slightly higher than that of the ABR system, indicating that the MFC of the coupled system can effectively assist the ABR. The first cell showed the highest removal efficiency of dyes, suggesting that most of the macromolecular organic compounds were degraded by hydrolytic acidifying bacteria present in the first cell.[30] As can be seen from Figure 2e, the COD concentration is gradually decreased with the direction of water flow in the cell. As the first cell size of the reactor is 1.5 times larger than that of other cells, the hydraulic load and the concentration of toxic and harmful substances are the largest, which may also be the reason for the minimum power density and current density of the first cell. The power density of the second cell is the highest because the dye is mainly degraded in the first cell and the toxicity is reduced, which results in the second cell having both adequate nutrient supply and relatively low toxicity compared to other cells. Although the COD concentration in the third cell is greater than that in the fourth cell, the dye concentration in the fourth cell is lower than that in the third cell, that is, the toxicity is lower than that in the third cell, indicating that the toxicity of organic matter in the reactor has a greater impact on the power density than that of COD.

2.2. Quantitative Analysis of SMP and EPS. During the degradation of organic matter, a small part of the SMP matter constitutes an important fraction of the effluent chemical oxygen demand (COD) in the biological wastewater treatment process.[31] It can be seen from Figure 3 that the SMP protein, polysaccharide, and humic acid of the ABR-MFC system and the ABR system showed a decreasing trend along the process. However, the polysaccharide of SMP of the ABR system did not show an observable trend in which the concentration of each cell was the same. This indicates that the soluble proteins, humic acids, and polysaccharides in the system are easy to remove. On the other hand, the second cell shows the lowest value in the total concentration of SMP in the ABR system. It was speculated that the compounds with SMP influent produced after the second cell were degraded and biotransformed to produce new SMP. This could be because the rate of biotransformation was greater than the rate of degradation.[32]

https://doi.org/10.1021/acsomega.1c03560
ACS Omega 2021, 6, 23515−23527

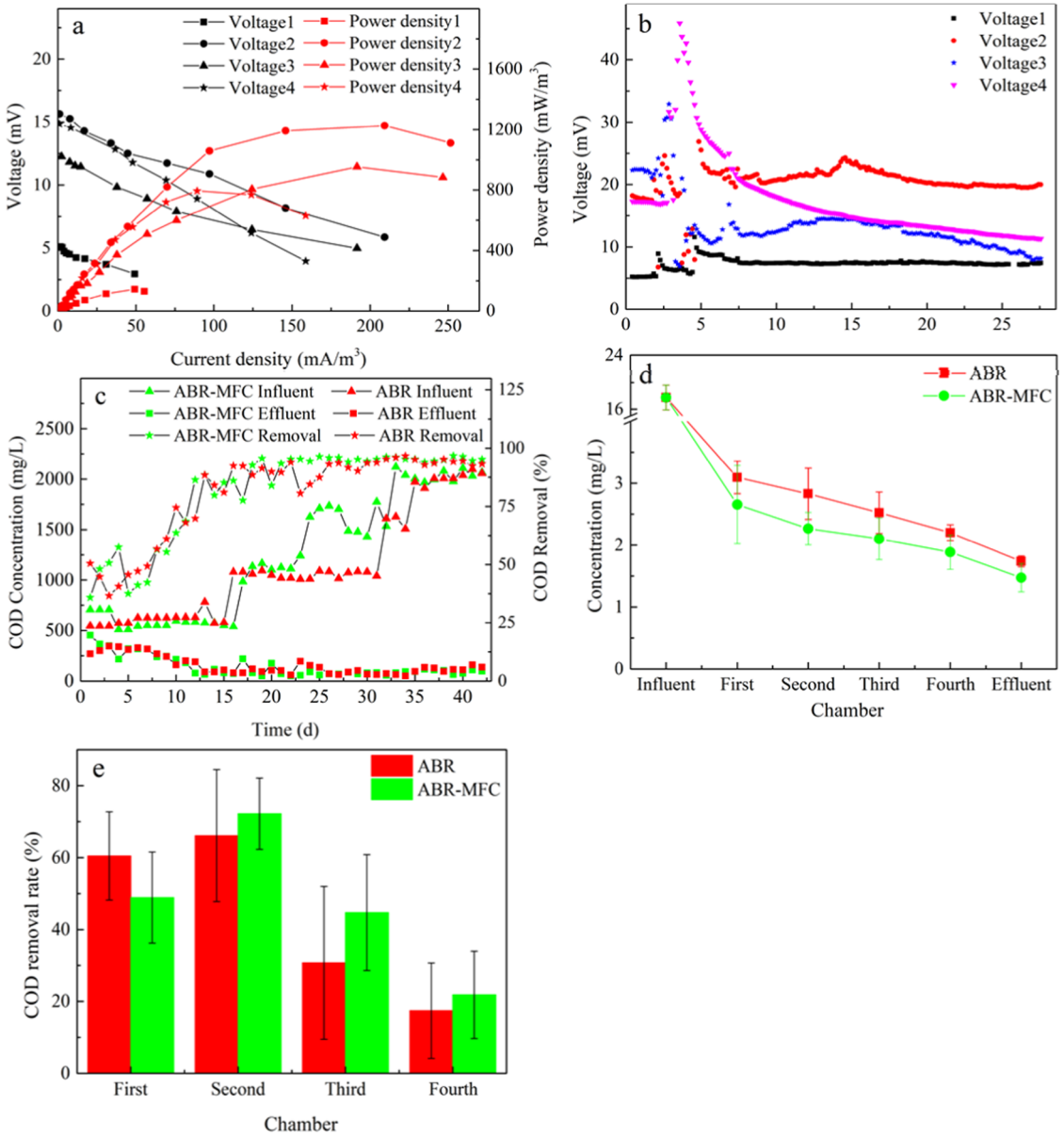

Figure 2. Power density of each cell of ABR-MFC (a), output voltage of ABR-MFC (b), chemical oxygen demand (COD) of each cell of ABR-MFC and ABR (c), dye concentration change diagram of each cell of ABR-MFC and ABR (d), and relative removal rate of COD in each chamber of ABR-MFC and ABR (e).

The EPS in sludge are the macromolecular substances secreted by microorganisms themselves.[33] As one of the important components of the bacterial micelle, the EPS plays a vital role in nutrient absorption, signal transmission, adsorption, and bridging, promoting the formation of granular sludge, maintaining its granular three-dimensional structural stability, and acting as a barrier to the cell.[34] LB-EPS showed stronger binding performance than TB-EPS. When bioadsorption and flocculation occurred simultaneously, LB-EPS was not only used as a chelating adsorbent but also as a flocculant to further improve its adsorption capacity.[35] As shown in Figure 3, the concentrations of proteins, polysaccharides, and humic acids of ABR-MFC LB-EPS were all greater than those of the ABR system, indicating that ABR-MFC has better adsorption capacity than the ABR system. Another finding reported that the levels of protein and polysaccharide in TB-EPS were significantly higher than that in LB-EPS in the formation process of granular sludge, indicating that the polysaccharide was an important component in forming the granular sludge skeleton.[36] The concentration of TB-EPS in the ABR-MFC and ABR systems was higher than that in LB-EPS, indicating that the two systems have a good capacity to produce granular sludge.

The aggregation capacity of the sludge hydrolyzed by polysaccharides (PSs) was significantly lower than that of sludge hydrolyzed by proteins (PNs), hence indicating that polysaccharides played a more important role in the structural construction of granular sludge.[37] Another study showed that the polysaccharides could maintain the outer structure of granular sludge, whereas proteins maintain their inner structure.[38] The newly discovered glycoproteins in EPS are also considered to be important for maintaining the granular structure of anammox.[39] For both LB-EPS and TB-EPS, the concentration of polysaccharides in the ABR-MFC system was

https://doi.org/10.1021/acsomega.1c03560
ACS Omega 2021, 6, 23515−23527

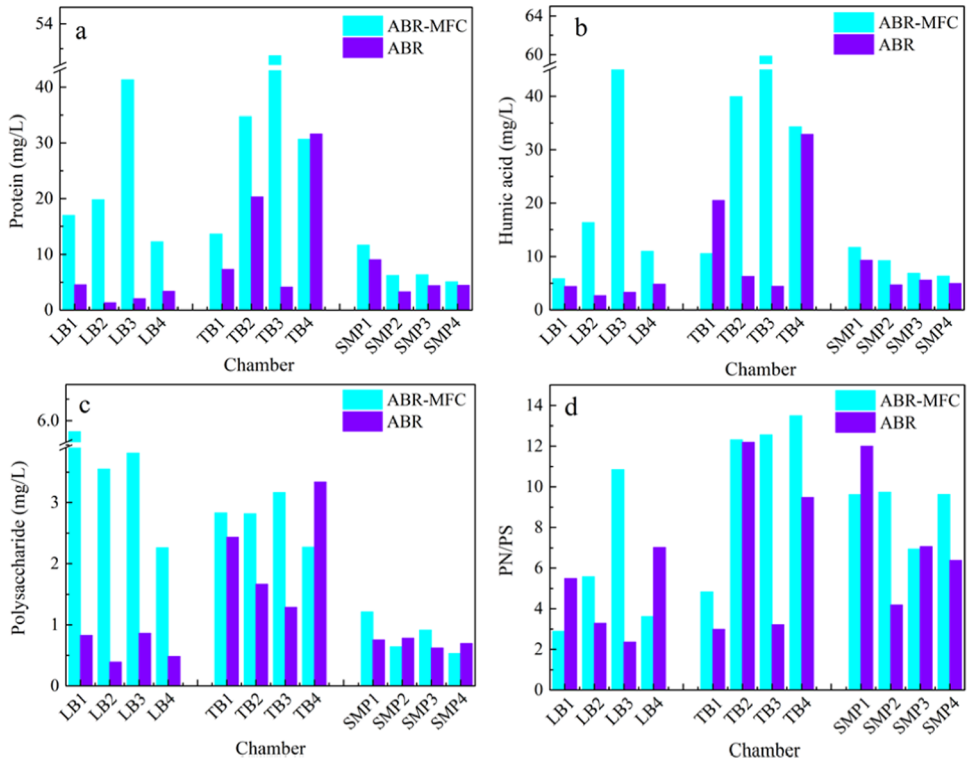

Figure 3. Protein (a), humic acid (b), polysaccharide (c), and ratio of protein to polysaccharide (d) of ABR-MFC and ABR.

higher than that in the ABR system, indicating that the stability of granular sludge structure in the ABR-MFC system was higher than that in a specific ABR system. The methane generated in the system can also stimulate the production of polysaccharides and contribute to the formation and stability of granular sludge. This could be done via the formation of a certain hydrodynamic shear during the process of rising in the reactor and under the hydrodynamic action in the reactor.

PN/PS is another important index to measure the degree of sludge granulation. It is known that the PN/PS increases with the progress of granulation. An increase in protein ratio can effectively reduce the electronegativity of the microbial cell surface, thus promoting sludge granulation.[40] As shown in Figure 3d, the ratio of PN/PS of the coupling system is generally higher than that of the ABR system regardless of EPS or SMP. EPS contains polysaccharides, proteins, and lipids that can be used as substrates for anaerobic fermentation. After the reaction by microorganisms, these substances are converted into humic acids. Since the activated sludge was obtained from the artificial water distribution in this experiment, the humic acid was added without additional substances in the latter experiment. The experiments in the SMP and EPS of humic acid were mainly derived from microbes themselves.[41]

Therefore, the internal state of the ABR-MFC reactor is more conducive to the formation of granular sludge. In addition, it was believed that the size of sludge particle was positively correlated with EPS,[42] this finding also concurred with the sludge particle size presented in the latter section

2.3. Fluorescence Spectroscopy Analysis. During the experiment, the simulated wastewater was passed through both the ABR and ABR-MFC coupling reactor. The SMP and EPS of the effluent from each cell of the reactor were diluted by 20 times before being subjected to fluorescence EEMS.[43] It can be seen from the figure that the organic matter in each cell contained six peaks, which can be divided into five regions according to Chen's classification method.[44] Since peak 1 is located in region IV, the organic matter is the soluble microbial product. The location of peak 2 in region I represents the characteristic peak of tyrosine protein while the location of peak 3 in region II represents the characteristic peak of tryptophan-like protein. Peak 4 is found in region III, indicating that the organic matter is fulvic acid like organics, whereas both peaks 5 and 6 found in region V could be assigned to the humic acid like organics.

It can be seen from Figure 4 that the fluorescence intensity of SMP-soluble microorganisms and humic acid like tyrosine protein corresponding to peak 6 in the ABR shows a decreasing trend by 43.9 and 12.9%, respectively. The tryptophan-like proteins, fulvic acid like organics, and humic acid like organics that correspond to peak 5 show an increasing trend. However, the fluorescence intensity of the SMP-soluble microorganisms and humic acids that correspond to peak 6 do not change significantly during the process in the ABR-MFC coupling reactor. The fluorescence intensity of tyrosine protein in SMP decreases gradually in the ABR-MFC coupling reactor, and the fluorescence intensity of tyrosine protein in each cell in the ABR-MFC coupling reactor is lower than that in the ABR. In addition, the fluorescence intensity of tryptophan-like proteins in SMP increases from the first cell to the fourth cell in the ABR-MFC coupling reactor, but the increment rate in the ABR-MFC reactor was less than that in the ABR. It was also found that the fluorescence intensity of the fulvic acid like organics in the SMP and the humic acid like organics corresponding to peak 5 in the ABR-MFC coupling reactor decreases during the process.

Overall, the above findings above revealed that the ABR-MFC coupling reactor can effectively degrade or inhibit the pollution of protein organic matter, remove fulvic acid like

https://doi.org/10.1021/acsomega.1c03560
ACS Omega 2021, 6, 23515−23527

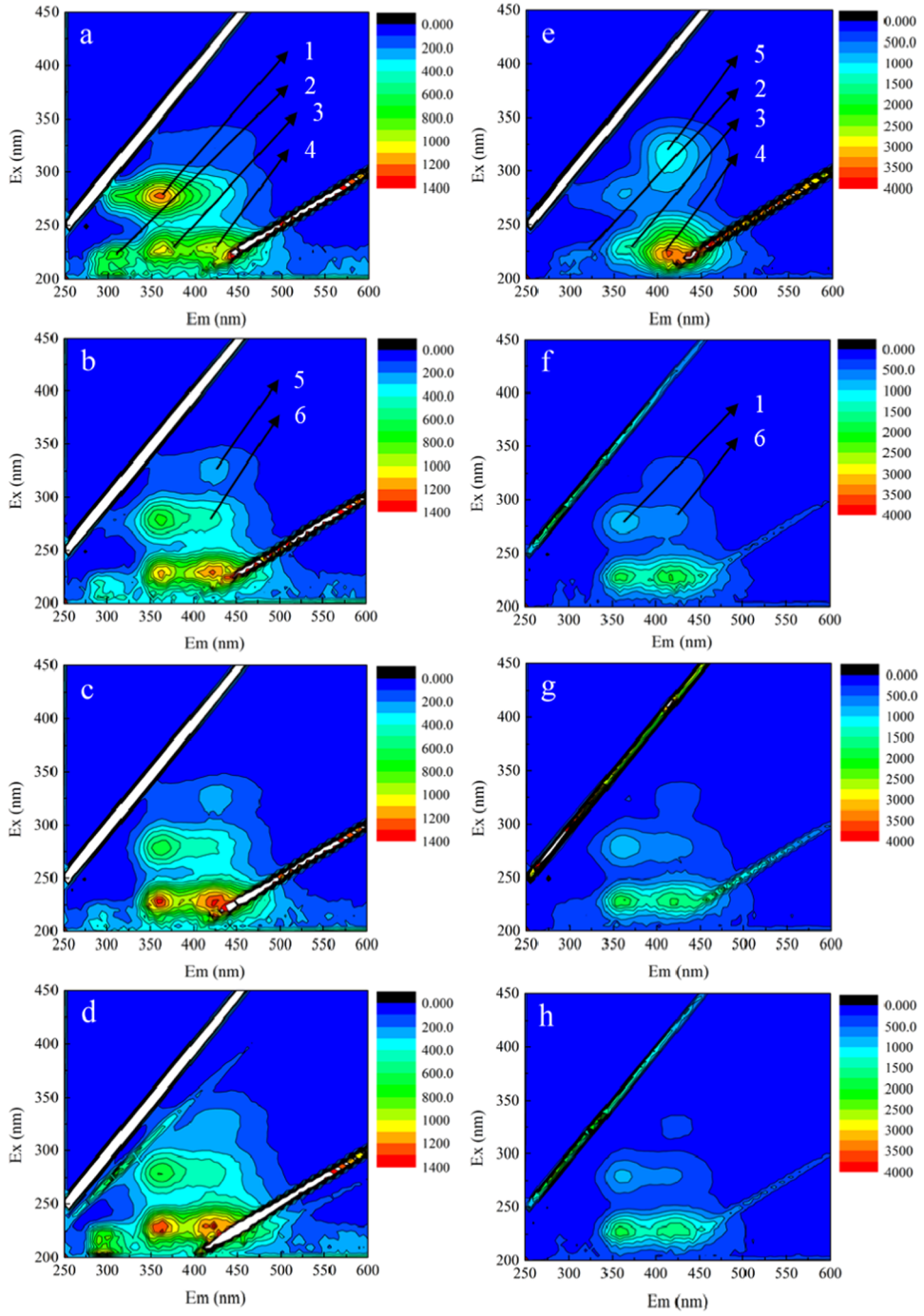

Figure 4. (a–d) EEM fluorescence spectrum study of the sludge SMP in the ABR. (e–h) EEM fluorescence spectrum study of sludge SMP in the ABR-MFC reactor.

organics and humic acid like organic matter under the action of a long-term low electric field.[45] As can be seen from Figures 5 and 6, the LB-EPS in the ABR-MFC coupling system is larger than the corresponding fluorescence intensity of each cell and each characteristic organic matter in the ABR system. In addition, the fluorescence peaks of each characteristic organic matter in each cell of TB-EPS in the two proposed systems were slightly stronger than those in the ABR system, indicating the higher concentrations of fluorescent substances in TB and LB in ABR-MFC. Compared with the ABR system, the fluorescence peaks corresponding to each component in LB show a blue-shift in the emission wavelength, a similar observation was reported by related researchers. Peak 1 could be related to the reduction of functional groups or the decomposition of aromatic groups or the breaking of macromolecular substances into small-molecule substances.[46,47] Therefore, the organic matter in the ABR-MFC system may be decomposed and utilized by microorganisms.

2.4. SEM Image of Granular Sludge. Figure 7a–d,e–h illustrates the SEM images of the activated sludge from compartment 1 to compartment 4 of the ABR system and the ABR-MFC system, respectively. As shown in Figure 7a,e, the activated sludge of filamentous bacteria is relatively abundant within the interior of the ABR system where it contains a

https://doi.org/10.1021/acsomega.1c03560
ACS Omega 2021, 6, 23515−23527

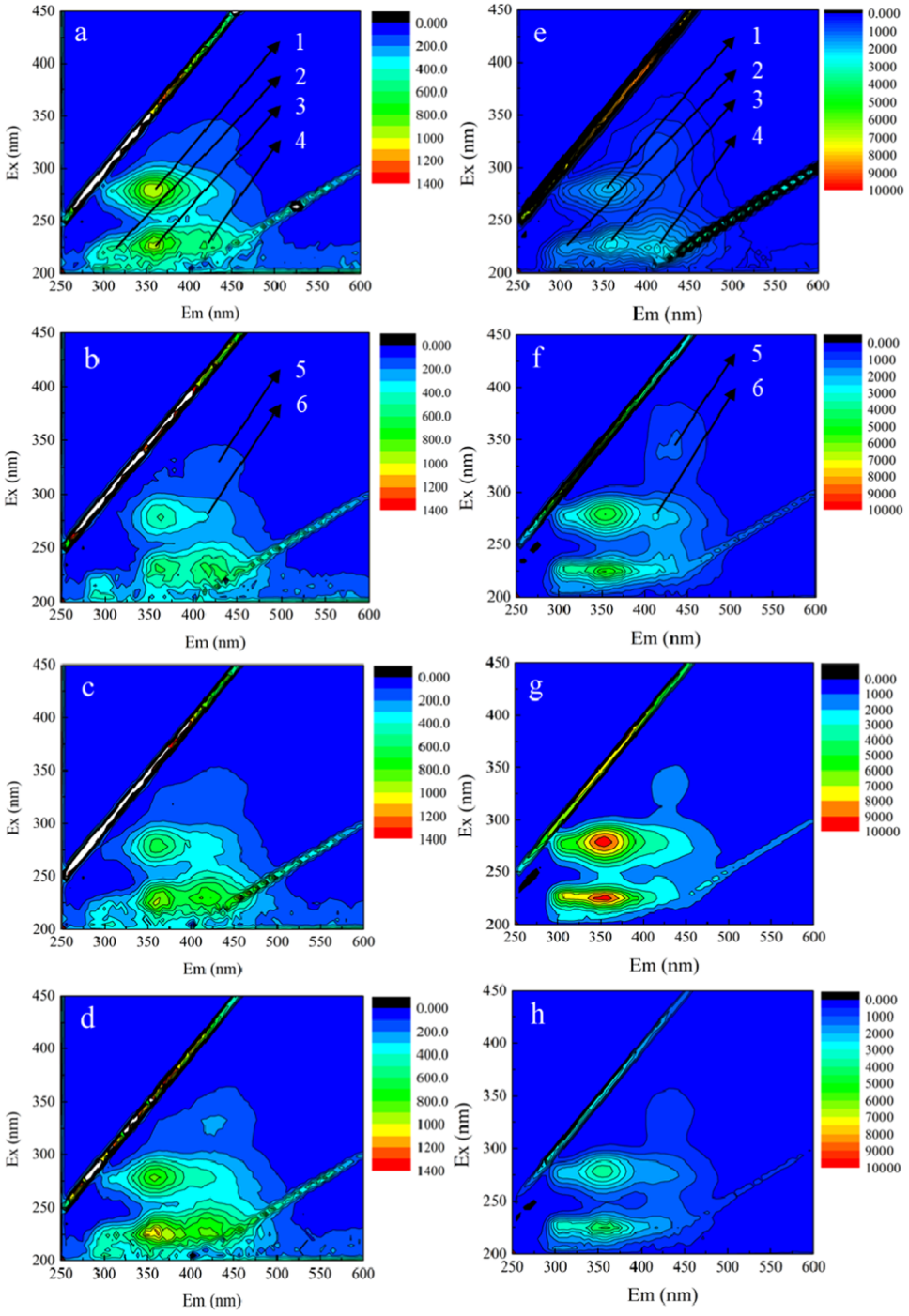

Figure 5. (a–d) EEM fluorescence spectrum study of sludge LB-EPS in the ABR. (e–h) EEM fluorescence spectrum study of the sludge LB-EPS in the ABR-MFC reactor.

relatively small amount of bacillus and cocci. Since the ABR-MFC system was utilized in the room, the indoor microbial species could be more abundant than that in the ABR system containing bacillus and cocci, most of them could be filamentous bacteria (zoogloea backing). Bacilli and cocci also inhabit the site reaction since there are well-defined micropores, holes, and channels that could serve as transport routes for substrates and nutrients. In Figure 7a,c,d,f–h, the filamentous bacteria were still dominant in the activated sludge of the ABR system while a small number of bacilli and cocci were attached to the skeleton constructed by filamentous bacteria. On the contrary, both filamentous bacteria and cocci were the main microorganisms found within the whole activated sludge associated with a small number of bacilli decorated on the castles in the ABR-MFC system. The activated sludge of the ABR-MFC system possessed a denser structure, abundant bacterial flora, and a large number of extracellular polymers characterized with a smooth, round, and dense structure. Coccus and bacillus are adhered to the surface of granular sludge by extracellular polymers.

It was found that the large number of EPS on the surface of sludge was significant for the adsorption and fixation of bacterial micelles. The small flocs would be formed by granular sludge as a result the sludge flocs in the liquid phase could be

https://doi.org/10.1021/acsomega.1c03560
ACS Omega 2021, 6, 23515−23527

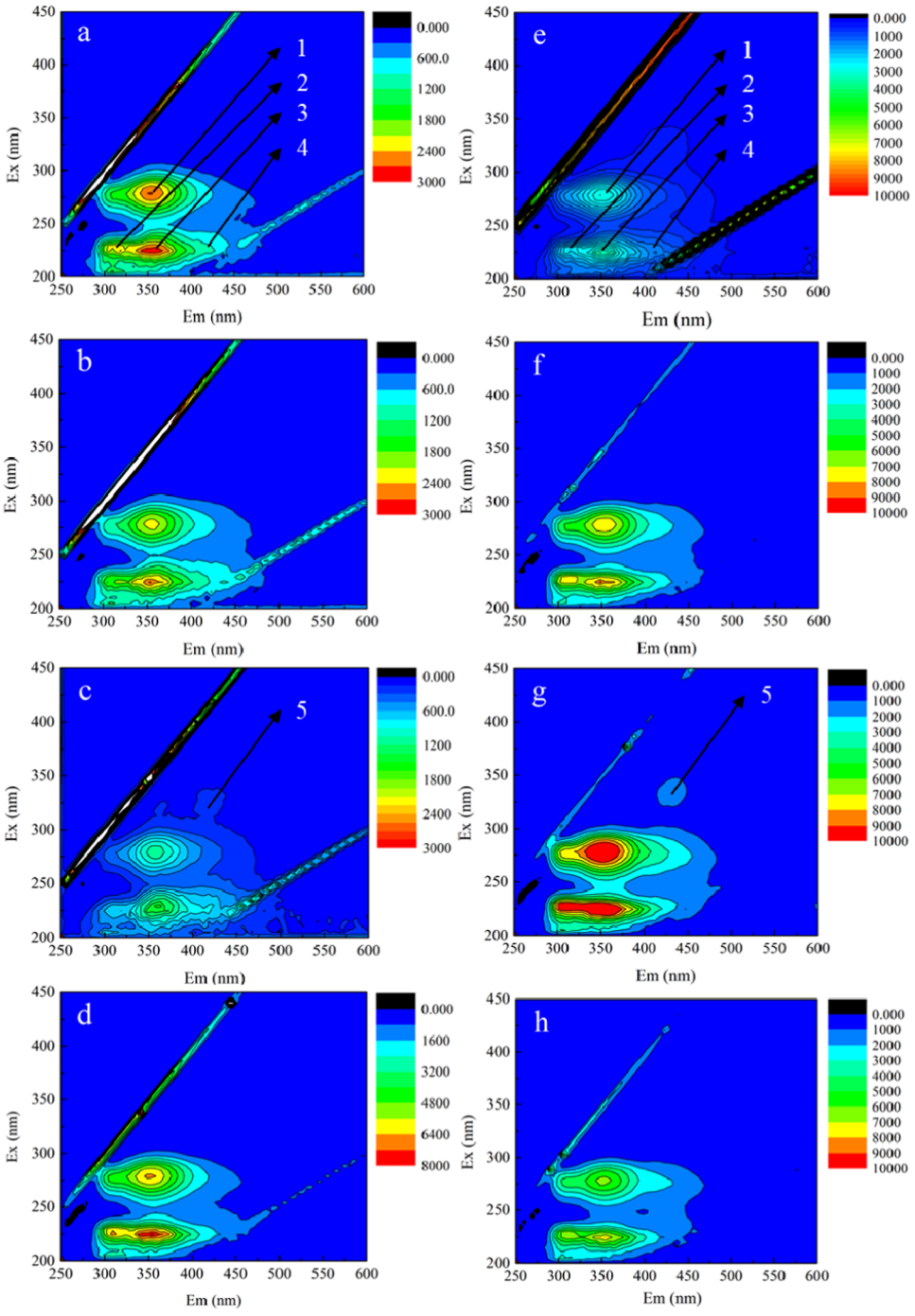

Figure 6. (a−d) EEM fluorescence spectrum study of sludge TB-EPS in the ABR. (e−h) EEM fluorescence spectrum study of sludge TB-EPS in ABR-MFC reactor.

reduced.[48] As the cell moved backward, the microorganism of various forms decreased progressively where the least amount of microorganism was found in the fourth cell of the two systems. This phenomenon may be due to the decrease in the pollutant concentration along the reactor. To sum up, the MFC system can effectively reduce the toxicity of dye wastewater and promote the growth and development of microorganisms in the coupling system.

2.5. Sludge Particle Size. The particle size of the sludge can reflect the state of granular sludge inside the reactor and the toxicity of organic matter inside the reactor. It can be seen from Figure 8 that the average particle size of the ABR-MFC system from the first cell to the fourth cell was within the range of 119.974−452.341 μm while the average particle size of the ABR system from the first cell to the fourth cell was 12.378−177.912 μm. The sludge particle size in the first cell of the ABR-MFC system shows two normal distribution trends. The sludge particle size detected in the system was uniformly distributed between 5.207−239.780 and 351.670−3080.544 μm, presenting the stratification phenomenon of sludge particle size. In the ABR system, the sludge particle size in the second cell was evenly distributed between 2.75−58.88 and 66.897−351.670 μm in which the sludge particle size stratification phenomenon was also observed. Such an

https://doi.org/10.1021/acsomega.1c03560
ACS Omega 2021, 6, 23515−23527

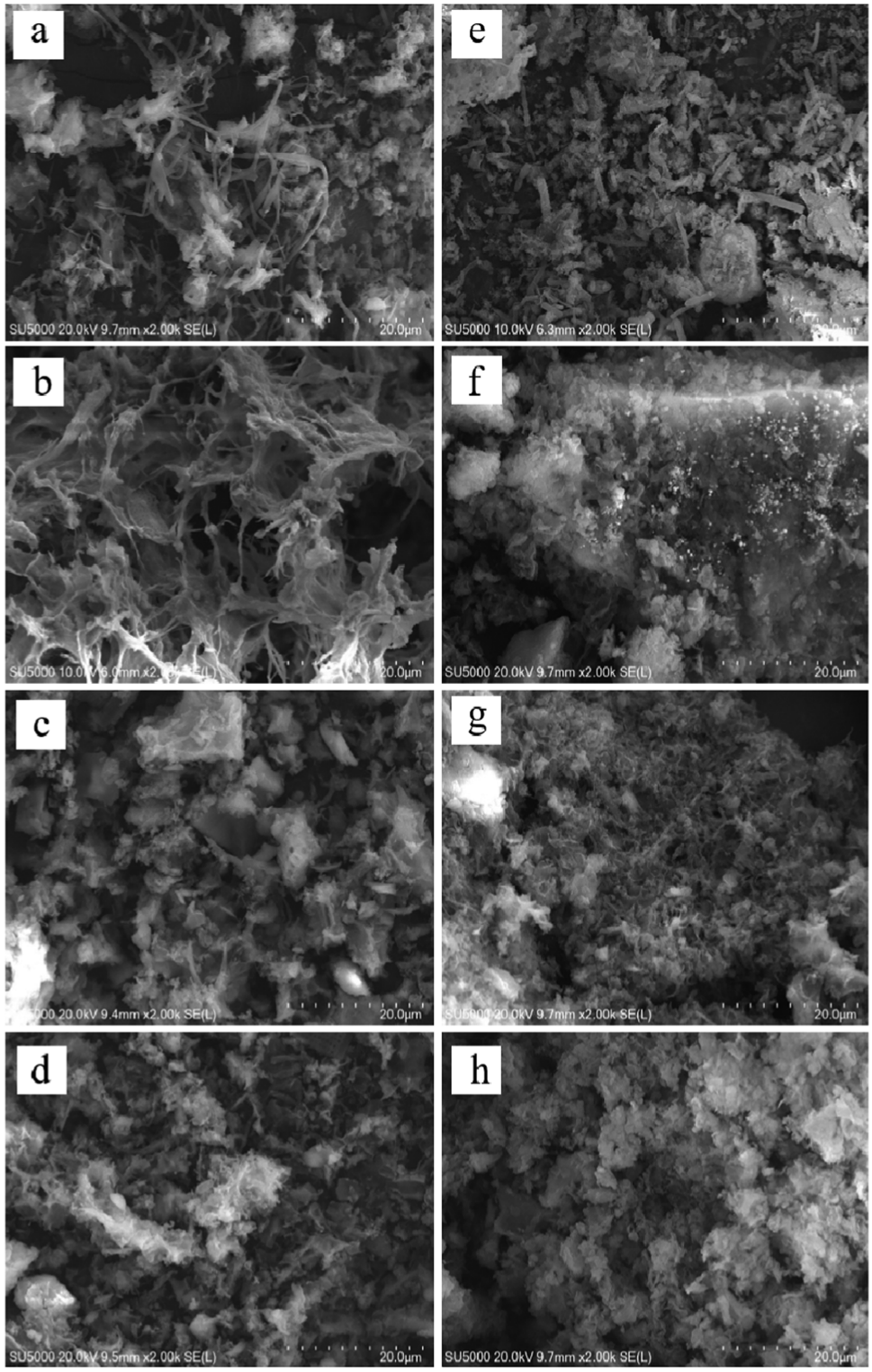

Figure 7. (a–d) SEM images of granular sludge in the ABR from the first compartment to the fourth compartment. (e–h) SEM images of granular sludge in the ABR-MFC reactor from the first compartment to the fourth compartment.

observation could be due to the utilization of different sources of the added sludge. This phenomenon was formed under the action of complex hydraulic conditions in the reactor; the production of a small amount of white granular sludge was speculated to be anaerobic and denitrifying granular sludge.[49]

It can be seen that the sludge particle size of each cell in the ABR-MFC system was slightly larger than that in the ABR system, attributed to the formation of the EPS microorganism particles. It is speculated that the sludge with a larger particle size would have a higher EPS content. This finding is consistent with the literature where the EPS content of the ABR-MFC system obtained was higher than that of the ABR system.[50−52] Moreover, the particle size of the sludge in the two systems decreased from the first compartment to the

https://doi.org/10.1021/acsomega.1c03560
ACS Omega 2021, 6, 23515−23527

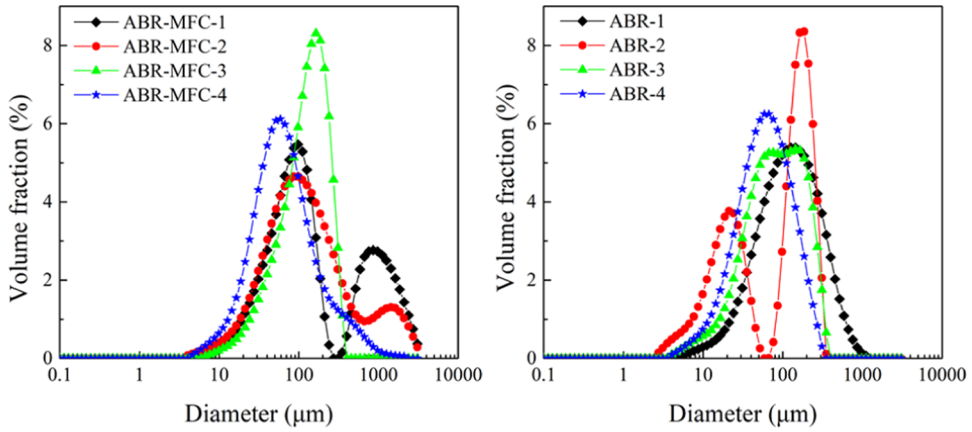

Figure 8. Sludge particle size distribution of activated sludge in chamber 1 to chamber 4 of the ABR and the ABR-MFC reactor.

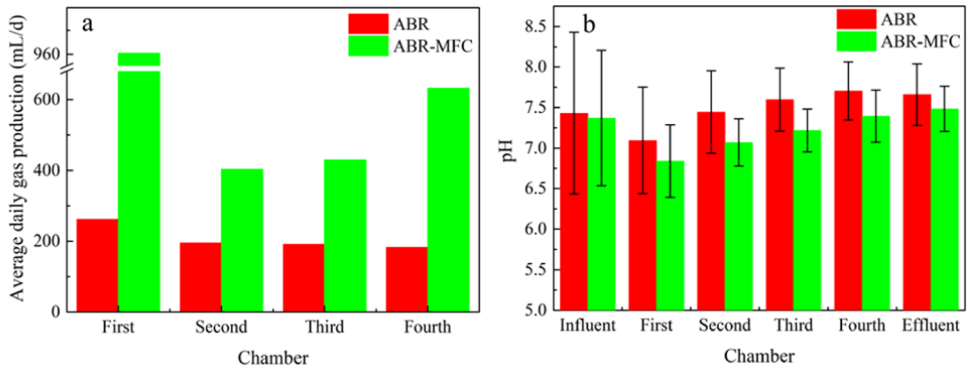

Figure 9. Methane production (a) and pH changes (b) in the ABR and ABR-MFC reactor from compartments 1 to 4.

fourth compartment. In both systems, the first compartment forms the largest size of granular sludge because the sludge in the front compartment grew faster and formed granules with sufficient nutrition. On top of that, the smaller the particle size of sludge particles in the compartment, the larger the specific gravity due to the lack of nutrients in the latter compartment. Combined with the hydraulic shear effect, the anaerobic sludge is difficult to agglomerate into larger particles. It was also found that the granular sludge particle size is smaller than the coupling of sludge in the reactor that resulted from the inhibition of toxicity in dye wastewater in the ABR system. Overall, this shows that the MFC can effectively reduce the toxicity of dye wastewater and promote the formation of granular sludge in the coupled systems.

2.6. Methane Production. Methane production reflects the anaerobic state inside the reactor. As observed from Figure 9a that the average daily methane production of each cell in the ABR-MFC system was significantly higher than that of the ABR, indicating that MFC improved the methane production rate in the coupled reactor. For the two-reactor system, the gas production in the first compartment was greater than that found by other researchers. This was because the experimental volume of the reactor chamber of the first compartment was 1.5 times larger than that of the others, hence a relatively long residence time of wastewater was needed. As a result, more poisonous and harmful substances can be removed in the first compartment compared with others. The organic load and gas production of the first compartment was increased, which subsequently reduced the amount of harmful substances in the subsequent compartments. In addition, it should be noted that the methane production in both systems was much lower than the theoretical value, which may be attributed to the lower SRT (7d) used since SRT greater than 8d could better promote methane production.[53] However, the gas production of the fourth cell in the coupled system was greater than that of the third cell and the second cell, which is consistent with the results of other researchers. Overall, the gas production of the last three cells in the ABR showed insignificant differences.

It can be seen from Figure 9b that the pH dropped to the lowest level in the first cell and then rose along the process due to the occurrence of hydrolysis and acidification in the first cell.[54] During the process of anaerobic acid production, the pH in the reactor was reduced with the accumulation of VFA. The changes in pH affected the different stages of anaerobic fermentation including hydrolysis, acidification, and methanation. When the pH range was within 5.0−6.5, the hydrolysis of organic matter could be promoted while inhibiting the activity of methanogens. When a higher pH (more than 6.5) was adopted, a methanation reaction would be preferable.[55−57] In this experiment, the pH of each cell in the two reactors was greater than 6.5, hence it was conducive to the generation of methane.

3. CONCLUSIONS

This study demonstrates valuable information for improving the removal efficiency of dye wastewater and the antitoxicity of activated sludge as well as the recovery of energy. Both the ABR-MFC reactor and ABR showed a longer HRT of 48 h and a maximum power density of 1226.43 mW/m^3 in the second cell. It was found that the EPS content, sludge particle size, methane production, and microbial quantity in the ABR-MFC

https://doi.org/10.1021/acsomega.1c03560
ACS Omega 2021, 6, 23515−23527

reactor were better than those in the ABR. It was also revealed from the findings that ABR-MFC performed better in terms of the treatment of dye wastewater, cultivation of high-quality granular sludge, and the generation of electricity. Overall, the results obtained in this study provide a possibility to scale up the coupled reactor for practical application in the treatment of dye wastewater.

4. MATERIALS AND METHODS

4.1. Preparation of Wastewater. The printing and dyeing wastewater used in this experiment was simulated based on the contents of effluent from the Hebei Sanli Group. This includes cationic azo dye, anthraquinone, glacial acetic acid, dyeing agent, defoaming agent, and other additives. The treatment of simulated wastewater was performed under a hydraulic retention time of 48 h to investigate the difference between the ABR-MFC coupling system and the ABR. The simulated wastewater contained 2000 mg/L sucrose, 300 mg/L NH_4Cl, 20 mg/L KH_2PO_4, 1200 mg/L $NaHCO_3$, 30 mg/L $MgSO_4{\cdot}7H_2O$, 20 mg/L $CaCl_2{\cdot}2H_2O$, and 20 mg/L Eriochrome Red B (Aladdin AR solid state). Then, 1 mg/L trace element solution was added to the simulated wastewater. Sodium bicarbonate was used to adjust the pH value between 8 and 9 to reach the pH of the water from Hebei Sanli Group. All chemicals used in this study were of analytical grade and used without further purification. At the beginning of the study, sucrose was used as the influent substrate to enhance the sludge activity. After that, the dye was gradually used as the substrate in the simulated wastewater.[26]

4.2. Configuration of ABR-MFC Coupling Reactor. The schematic diagram of the ABR-MFC coupling reactor is shown in Figure 1. The reactor was made of plexiglass with a thickness of 5 mm with an effective height of 30 cm and a volume of 30.7 L (length × width × height = 65 cm × 25 cm × 33 cm). The vertical baffle reactor was divided into four chambers by careful reduction (1 cm), the width ratio of the rising area and falling area of the water flow in the chamber was 4:1, and the volume of the first chamber was 1.5 times than that of the other chambers. The lower end of the folding plate leading to the upper chamber has a 45° chamber guide plate to distribute water. This was to ease the water being transported to the center of the upper chamber to mix with the muddy water; consequently, the upper chamber can be evenly distributed. Each cell has a 3 cm diameter hole at the top. The top of the reactor is completely closed only for methane collection while the 3 cm diameter hole is opened throughout the experiment. A sampling port is provided on the side, and a mud discharge port is provided at the bottom. Such an experimental setup was used to regularly sample and monitor the sludge in the reactor and the changes in water quality. The reactor was placed in the room. During the experiment, the reactor was initiated at a room temperature of 25 °C. Heating rods were placed in each cell at a constant temperature for thermal insulation.

The simulated wastewater was fed into the reactor through a peristaltic pump and the steady flow rate was controlled when passed through the four cells. The anode of the MFC used for the coupling reactor was a carbon brush (20 cm long and 5 cm in diameter), while the cathode was a rectangular carbon blanket. The dimension of the first cell was 20 × 20 cm while the others were 10 cm × 20 cm. The external resistor was a variable resistor with an initial value set at 1000 Ω. The voltage of the external resistor was recorded with a paperless recorder, and the voltage data obtained was stored in the paperless recorder. The anode was held in a cell with titanium wire and immersed in water, while the carbon felt cathode floats on the surface. The titanium wire was used to connect the anode and cathode. The experimental sludge used was collected from the oxidation ditch of Beijing Qinghe Reclaimed Water Plant and Beijing Gaobeidian Sewage Treatment Plant with a certain degree of domestication. The addition of sludge from different sources contributed to the enrichment of the sludge biome.

4.3. Extraction Process of Soluble Microbial Product (SMP) and EPS. The same amounts of sludge mixture from the two systems were taken out and centrifuged for 5 min under the centrifugal force of 3000 r/min. After the upper clarification solution was filtered by 0.45 μm filter membrane, the SMP was obtained. In this paper, the extraction of sludge EPS was adopted a step-by-step thermal extraction method. Initially, the preheated 0.05% NaCl solution (to 70 °C) was added to the remaining centrifugal tube after extraction of SMP. Then, it was suspended to the original volume, fully mixed under the centrifugal force of 3000 r/min for 10 min, the loosely bound EPS (LB-EPS) was obtained after the upper clarification solution was filtered by a 0.45 μm filter membrane. After that, the 0.05% NaCl solution was added to the remaining centrifuge tubes, suspended to the original volume, and fully mixed with the sludge mixture before being heated in a water bath at 60 °C for 30 min. The heated sludge mixture was cooled down, followed by centrifugation for 15 min under the centrifugal force of 3000 r/min. The tightly bound EPS (TB-EPS) of the sludge floc was obtained.[28]

4.4. Analyses and Calculations. A recorder (KSB1−24AOR, Ningbo, China) was used to monitor the output voltage of the external resistor every 1 min. The power density curve was measured in the range of 5−5000 Ω. According to the measured voltage at both ends of the external resistor and the resistance value of the external resistor, the current value can be calculated using Ohm's law as shown in the equation below:

$$I = \frac{U}{R} \tag{1}$$

where I is the current (mA), U is the voltage of the external resistor (mV), and R is the external resistor (Ω). The output voltage was used to calculate the power density of the system as shown in the equation below:

$$P_{An} = \frac{U^2}{R\ V_{An}} \tag{2}$$

where P_{An} is the volumetric power density (W/m^3) and V_{An} is the effective volume of the anode chamber.

The value of COD, absorbance of the dye, and chromaticity of the dye were measured every 48 h. Both COD and dye chromaticity were measured using the water quality speed meter (Sheng Aohua 6B-2000) while the absorbance of the dye was measured by an ultraviolet spectrophotometer; the maximum absorption wavelength of the dye was 465.5 nm (Persee, T6 New Century, Beijing). The Folin−Lowry method was used to measure the contents of protein and humic acid while the anthrone-sulfuric acid method was used to measure the polysaccharide. The sludge particle size was quantified by a super-high-speed intelligent particle size analyzer (Mastersizer 3000). The morphology of sludge and microorganism were observed by field emission scanning electron microscopy (Hitachi SU5000 + Oxford Instruments Ultim Max). The

https://doi.org/10.1021/acsomega.1c03560
ACS Omega 2021, 6, 23515−23527

excitation-emission matrix (EEM) spectra were detected by a Hitachi F-7000 fluorescence spectrometer. The excitation spectra were scanned in the range of 200−450 nm with a scanning interval of 5 nm. The emission wavelength used was in the range of 250−600 nm with a scanning interval of 2 nm.

AUTHOR INFORMATION

Corresponding Author

Yanbin Yun − *Beijing Key Laboratory of Water Source Control Technology, Sludge Disposal and Recycling Technology Laboratory, College of Environmental Science and Engineering, Beijing Forestry University, Beijing 100083, People's Republic of China;* orcid.org/0000-0003-2273-9220; Email: Yanbinyun@bjfu.edu.cn

Authors

Na Liu − *Beijing Key Laboratory of Water Source Control Technology, Sludge Disposal and Recycling Technology Laboratory, College of Environmental Science and Engineering, Beijing Forestry University, Beijing 100083, People's Republic of China;* orcid.org/0000-0002-6045-4165

Liming Hu − *Beijing Key Laboratory of Water Source Control Technology, Sludge Disposal and Recycling Technology Laboratory, College of Environmental Science and Engineering, Beijing Forestry University, Beijing 100083, People's Republic of China*

Linting Xin − *Beijing Key Laboratory of Water Source Control Technology, Sludge Disposal and Recycling Technology Laboratory, College of Environmental Science and Engineering, Beijing Forestry University, Beijing 100083, People's Republic of China*

Mengxia Han − *Beijing Key Laboratory of Water Source Control Technology, Sludge Disposal and Recycling Technology Laboratory, College of Environmental Science and Engineering, Beijing Forestry University, Beijing 100083, People's Republic of China*

Panyue Zhang − *Beijing Key Laboratory of Water Source Control Technology, Sludge Disposal and Recycling Technology Laboratory, College of Environmental Science and Engineering, Beijing Forestry University, Beijing 100083, People's Republic of China*

Complete contact information is available at: https://pubs.acs.org/10.1021/acsomega.1c03560

Author Contributions

Na Liu designed the experiment, executed this study, completed the data analysis, and wrote the first draft of the paper. Mengxia Han and Linting Xin participated in the experimental design. Liming Hu participated in the analysis of experimental results. Yanbin Yun was the project architect and leader and oversaw the experiment design, data analysis, paper writing, and revision. Panyue Zhang supervised the design and revision of the paper. All authors read and agreed on the final text.

Notes

The authors declare no competing financial interest.

ACKNOWLEDGMENTS

This work was supported by Studies on the Preparation of Super-hydrophobic and Superhydrophilic Films [grant number 200-661902043].

REFERENCES

(1) Cai, H.; Mei, Y.; Chen, J.; Wu, Z.; Lan, L.; Zhu, D. An analysis of the relation between water pollution and economic growth in China by considering the contemporaneous correlation of water pollutants. *J. Cleaner Prod.* **2020**, *276*, No. 122783.

(2) Cui, M.; Sangeetha, T.; Gao, L.; Wang, A. Efficient azo dye wastewater treatment in a hybrid anaerobic reactor with a built-in integrated bioelectrochemical system and an aerobic biofilm reactor: Evaluation of the combined forms and reflux ratio. *Bioresour. Technol.* **2019**, *292*, No. 122001.

(3) Assadi, A.; Naderi, M.; Mehrasbi, M. R. Anaerobic−aerobic sequencing batch reactor treating azo dye containing wastewater: effect of high nitrate ions and salt. *J. Water Reuse Desalin.* **2018**, *8*, 251−261.

(4) Chen, C.; Wang, G.; Tseng, I.; Chung, Y. Analysis of bacterial diversity and efficiency of continuous removal of Victoria Blue R from wastewater by using packed-bed bioreactor. *Chemosphere* **2016**, *145*, 17−24.

(5) Yuan, Y.; Ning, X.; Zhang, Y.; Lai, X.; Li, D.; He, Z.; Chen, X. Chlorobenzene levels, component distribution, and ambient severity in wastewater from five textile dyeing wastewater treatment plants. *Ecotoxicol. Environ. Saf.* **2020**, *193*, No. 110257.

(6) Deogaonkar, S. C.; Wakode, P.; Rawat, K. P. Electron beam irradiation post treatment for degradation of non biodegradable contaminants in textile wastewater. *Radiat. Phys. Chem.* **2019**, *165*, No. 108377.

(7) Liu, L.; Chen, Z.; Zhang, J.; Shan, D.; Wu, Y.; Bai, L.; Wang, B. Treatment of industrial dye wastewater and pharmaceutical residue wastewater by advanced oxidation processes and its combination with nanocatalysts: A review. *J. Water Process Eng.* **2021**, *42*, No. 102122.

(8) Wang, S.; Zhang, B.; Shan, C.; Yan, X.; Chen, H.; Pan, B. Occurrence and transformation of phosphonates in textile dyeing wastewater along full-scale combined treatment processes. *Water Res.* **2020**, *184*, No. 116173.

(9) Ji, G. D.; Sun, T. H.; Ni, J. R.; Tong, J. J. Anaerobic baffled reactor (ABR) for treating heavy oil produced water with high concentrations of salt and poor nutrient. *Bioresour. Technol.* **2009**, *100*, 1108−1114.

(10) Ali, J.; Wang, L.; Waseem, H.; Sharif, H. M. A.; Djellabi, R.; Zhang, C.; Pan, G. Bioelectrochemical recovery of silver from wastewater with sustainable power generation and its reuse for biofouling mitigation. *J. Cleaner Prod.* **2019**, *235*, 1425−1437.

(11) Silveira, G.; de Aquino Neto, S.; Schneedorf, J. M. Development, characterization and application of a low-cost single chamber microbial fuel cell based on hydraulic couplers. *Energy* **2020**, *208*, No. 118395.

(12) Pandey, P.; Shinde, V. N.; Deopurkar, R. L.; Kale, S. P.; Patil, S. A.; Pant, D. Recent advances in the use of different substrates in microbial fuel cells toward wastewater treatment and simultaneous energy recovery. *Appl. Energy* **2016**, *168*, 706−723.

(13) Pant, D.; Arslan, D.; Van Bogaert, G.; Gallego, Y. A.; De Wever, H.; Diels, L.; Vanbroekhoven, K. Integrated conversion of food waste diluted with sewage into volatile fatty acids through fermentation and electricity through a fuel cell. *Environ. Technol.* **2013**, *34*, 1935−45.

(14) Patil, S. A.; Hägerhäll, C.; Gorton, L. *Electron Transfer Mechanisms between Microorganisms and Electrodes in Bioelectrochemical Systems*; Springer International Publishing: Cham, 2013; pp 71−129.

(15) Li, X.; Abu-Reesh, I.; He, Z. Development of Bioelectrochemical Systems to Promote Sustainable Agriculture. *Agriculture* **2015**, *5*, 367−388.

(16) Yoshizawa, T.; Miyahara, M.; Kouzuma, A.; Watanabe, K. Conversion of activated-sludge reactors to microbial fuel cells for wastewater treatment coupled to electricity generation. *J. Biosci. Bioeng.* **2014**, *118*, 533−539.

(17) Yang, Y.; Luo, O.; Kong, G.; Wang, B.; Li, X.; Li, E.; Li, J.; Liu, F.; Xu, M. Deciphering the Anode-Enhanced Azo Dye Degradation in Anaerobic Baffled Reactors Integrating With Microbial Fuel Cells. *Front. Microbiol.* **2018**, *9*, No. 2117.

(18) Liu, J.; Tian, C.; Jia, X.; Xiong, J.; Dong, S.; Wang, L.; Bo, L. The brewery wastewater treatment and membrane fouling mitigation strategies in anaerobic baffled anaerobic/aerobic membrane bioreactor. *Biochem. Eng. J.* **2017**, *127*, 53−59.
(19) Liu, H.; Lv, Y.; Xu, S.; Chen, Z.; Lichtfouse, E. Configuration and rapid start-up of a novel combined microbial electrolytic process treating fecal sewage. *Sci. Total Environ.* **2020**, *705*, No. 135986.
(20) Gul, H.; Raza, W.; Lee, J.; Azam, M.; Ashraf, M.; Kim, K. Progress in microbial fuel cell technology for wastewater treatment and energy harvesting. *Chemosphere* **2021**, *281*, No. 130828.
(21) Li, H.; Zuo, W.; Tian, Y.; Zhang, J.; Di, S.; Li, L.; Su, X. Simultaneous nitrification and denitrification in a novel membrane bioelectrochemical reactor with low membrane fouling tendency. *Environ. Sci. Pollut. Res.* **2017**, *24*, 5106−5117.
(22) Niu, Y.; Liu, X.; Chang, G.; Guo, Q. Treatment of isopropanol wastewater in an anaerobic fluidized bed microbial fuel cell filled with macroporous adsorptive resin as multifunctional biocarrier. *Sci. Total Environ.* **2020**, *719*, No. 137495.
(23) Xie, B.; Liu, B.; Yi, Y.; Yang, L.; Liang, D.; Zhu, Y.; Liu, H. Microbiological mechanism of the improved nitrogen and phosphorus removal by embedding microbial fuel cell in Anaerobic−Anoxic−Oxic wastewater treatment process. *Bioresour. Technol.* **2016**, *207*, 109−117.
(24) Oon, Y.; Ong, S.; Ho, L.; Wong, Y.; Oon, Y.; Lehl, H. K.; Thung, W. Innovative baffled microbial fuel cells for azo dye degradation: Interactive mechanisms of electron transport and degradation pathway. *J. Cleaner Prod.* **2021**, *295*, No. 126366.
(25) Saeed, T.; Jihad Miah, M. Organic matter and nutrient removal in tidal flow-based microbial fuel cell constructed wetlands: Media and flood-dry period ratio. *Chem. Eng. J.* **2021**, *411*, No. 128507.
(26) Tabassum, N.; Islam, N.; Ahmed, S. Progress in microbial fuel cells for sustainable management of industrial effluents. *Process Biochem.* **2021**, *106*, 20−41.
(27) Wagner, J.; Weissbrodt, D. G.; Manguin, V.; Ribeiro Da Costa, R. H.; Morgenroth, E.; Derlon, N. Effect of particulate organic substrate on aerobic granulation and operating conditions of sequencing batch reactors. *Water Res.* **2015**, *85*, 158−166.
(28) Li, X. Y.; Yang, S. F. Influence of loosely bound extracellular polymeric substances (EPS) on the flocculation, sedimentation and dewaterability of activated sludge. *Water Res.* **2007**, *41*, 1022−1030.
(29) Su, C.; Deng, Q.; Lu, Y.; Qin, R.; Chen, S.; Wei, J.; Chen, M.; Huang, Z. Effects of hydraulic retention time on the performance and microbial community of an anaerobic baffled reactor-bioelectricity Fenton coupling reactor for treatment of traditional Chinese medicine wastewater. *Bioresour. Technol.* **2019**, *288*, No. 121508.
(30) Wu, H.; Wang, S.; Kong, H.; Liu, T.; Xia, M. Performance of combined process of anoxic baffled reactor-biological contact oxidation treating printing and dyeing wastewater. *Bioresour. Technol.* **2007**, *98*, 1501−1504.
(31) Izadi, P.; Izadi, P.; Eldyasti, A. Holistic insights into extracellular polymeric substance (EPS) in anammosx bacterial matrix and the potential sustainable biopolymer recovery: A review. *Chemosphere* **2021**, *274*, No. 129703.
(32) Soh, Y. N. A.; Kunacheva, C.; Webster, R. D.; Stuckey, D. C. Composition and biotransformational changes in soluble microbial products (SMPs) along an anaerobic baffled reactor (ABR). *Chemosphere* **2020**, *254*, No. 126775.
(33) He, Q.; Zhou, J.; Wang, H.; Zhang, J.; Wei, L. Microbial population dynamics during sludge granulation in an A/O/A sequencing batch reactor. *Bioresour. Technol.* **2016**, *214*, 1−8.
(34) Wang, B.; Peng, D.; Hou, Y.; Li, H.; Pei, L.; Yu, L. The important implications of particulate substrate in determining the physicochemical characteristics of extracellular polymeric substances (EPS) in activated sludge. *Water Res.* **2014**, *58*, 1−8.
(35) Sun, X.; Wang, S.; Zhang, X.; Paul Chen, J.; Li, X.; Gao, B.; Ma, Y. Spectroscopic study of Zn2+ and Co2+ binding to extracellular polymeric substances (EPS) from aerobic granules. *J. Colloid Interface Sci.* **2009**, *335*, 11−17.
(36) Xu, J.; Pang, H.; He, J.; Wang, M.; Nan, J.; Li, L. Enhanced aerobic sludge granulation by applying carbon fibers as nucleating skeletons. *Chem. Eng. J.* **2019**, *373*, 946−954.
(37) Wang, S.; Huang, X.; Liu, L.; Shen, Y.; Yan, P.; Chen, Y.; Guo, J.; Fang, F. Understanding the mechanism in aggregation ability between aerobic and anammox granular sludge from the perspective of exopolysaccharides. *J. Water Process Eng.* **2020**, *38*, No. 101629.
(38) Liang, Z.; Tu, Q.; Su, X.; Yang, X.; Chen, J.; Chen, Y.; Li, H.; Liu, C.; He, Q. Formation, extracellular polymeric substances, and structural stability of aerobic granules enhanced by granular activated carbon. *Environ. Sci. Pollut.* **2019**, *26*, 6123−6132.
(39) Boleij, M.; Pabst, M.; Neu, T. R.; van Loosdrecht, M. C. M.; Lin, Y. Identification of Glycoproteins Isolated from Extracellular Polymeric Substances of Full-Scale Anammox Granular Sludge. *Environ. Sci. Technol.* **2018**, *52*, 13127−13135.
(40) Wei, D.; Wang, Y.; Wang, X.; Li, M.; Han, F.; Ju, L.; Zhang, G.; Shi, L.; Li, K.; Wang, B.; Du, B.; Wei, Q. Toxicity assessment of 4-chlorophenol to aerobic granular sludge and its interaction with extracellular polymeric substances. *J. Hazard. Mater.* **2015**, *289*, 101−107.
(41) Burdon, J. Are the Traditional Concepts of the Structures of Humic Substances Realistic? *Soil Sci.* **2001**, *166*, 752−769.
(42) Tian, Y.; Li, H.; Li, L.; Su, X.; Lu, Y.; Zuo, W.; Zhang, J. In-situ integration of microbial fuel cell with hollow-fiber membrane bioreactor for wastewater treatment and membrane fouling mitigation. *Biosens. Bioelectron.* **2015**, *64*, 189−195.
(43) Chen, W.; Yu, H. Advances in the characterization and monitoring of natural organic matter using spectroscopic approaches. *Water Res.* **2021**, *190*, No. 116759.
(44) Chen, W.; Westerhoff, P.; Leenheer, J. A.; Booksh, K. Fluorescence Excitation−Emission Matrix Regional Integration to Quantify Spectra for Dissolved Organic Matter. *Environ. Sci. Technol.* **2003**, *37*, 5701−5710.
(45) Li, H.; Tian, Y.; Zuo, W.; Zhang, J.; Pan, X.; Li, L.; Su, X. Electricity generation from food wastes and characteristics of organic matters in microbial fuel cell. *Bioresour. Technol.* **2016**, *205*, 104−110.
(46) Świetlik, J.; Dąbrowska, A.; Raczyk-Stanisławiak, U.; Nawrocki, J. Reactivity of natural organic matter fractions with chlorine dioxide and ozone. *Water Res.* **2004**, *38*, 547−558.
(47) Wang, Z.; Tang, S.; Zhu, Y.; Wu, Z.; Zhou, Q.; Yang, D. Fluorescent dissolved organic matter variations in a submerged membrane bioreactor under different sludge retention times. *J. Membr. Sci.* **2010**, *355*, 151−157.
(48) Liu, X.; Liu, J.; Deng, D.; Li, R.; Guo, C.; Ma, J.; Chen, M. Investigation of extracellular polymeric substances (EPS) in four types of sludge: Factors influencing EPS properties and sludge granulation. *J. Water Process. Eng.* **2021**, *40*, No. 101924.
(49) Cao, S.; Peng, Y.; Du, R.; Zhang, H. Characterization of partial-denitrification (PD) granular sludge producing nitrite: Effect of loading rates and particle size. *Sci. Total Environ.* **2019**, *671*, 510−518.
(50) Deng, S.; Wang, L.; Su, H. Role and influence of extracellular polymeric substances on the preparation of aerobic granular sludge. *J. Environ. Manage.* **2016**, *173*, 49−54.
(51) Sheng, G.; Yu, H.; Li, X. Extracellular polymeric substances (EPS) of microbial aggregates in biological wastewater treatment systems: A review. *Biotechnol. Adv.* **2010**, *28*, 882−894.
(52) Franca, R. D. G.; Pinheiro, H. M.; van Loosdrecht, M. C. M.; Lourenço, N. D. Stability of aerobic granules during lon g-term bioreactor operation. *Biotechnol. Adv.* **2018**, *36*, 228−246.
(53) Luo, J.; Feng, L.; Zhang, W.; Li, X.; Chen, H.; Wang, D.; Chen, Y. Improved production of short-chain fatty acids from waste activated sludge driven by carbohydrate addition in continuous-flow reactors: Influence of SRT and temperature. *Appl. Energy* **2014**, *113*, 51−58.
(54) Wu, H.; Wang, S.; Kong, H.; Liu, T.; Xia, M. Performance of combined process of anoxic baffled reactor-biological contact oxidation treating printing and dyeing wastewater. *Bioresour. Technol.* **2007**, *98*, 1501−1504.

https://doi.org/10.1021/acsomega.1c03560
ACS Omega 2021, 6, 23515−23527

(55) Fang, H. H.; Liu, H. Effect of pH on hydrogen production from glucose by a mixed culture. *Bioresour. Technol.* **2002**, *82*, 87−93.
(56) Xu, S. Y.; Karthikeyan, O. P.; Selvam, A.; Wong, J. W. C. Effect of inoculum to substrate ratio on the hydrolysis and acidification of food waste in leach bed reactor. *Bioresour. Technol.* **2012**, *126*, 425−430.
(57) Yuan, H.; Chen, Y.; Zhang, H.; Jiang, S.; Zhou, Q.; Gu, G. Improved Bioproduction of Short-Chain Fatty Acids (SCFAs) from Excess Sludge under Alkaline Conditions. *Environ. Sci. Technol.* **2006**, *40*, 2025−2029.

https://doi.org/10.1021/acsomega.1c03560
ACS Omega 2021, 6, 23515−23527